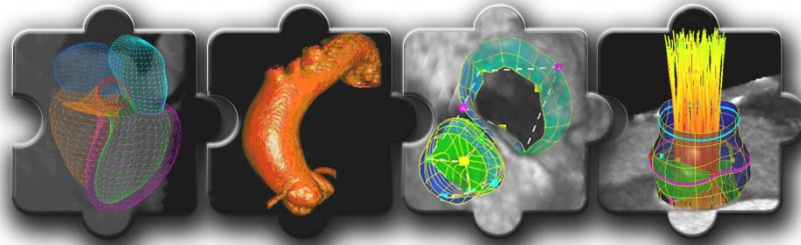


	D5.2 Left Heart Model Extension	Sim-e-Child FP7-ICT-2009-4 (SeC)
--	---------------------------------	-------------------------------------

**FP7-ICT-2009-4 (248421)
SeC
Sim-e-Child**



Collaboration Project

Thematic Priority: ICT

**Deliverable D5.2
Left Heart Model Extension**

Due date of delivery: 31 August 2011
Actual submission date: 31 August 2011

Start date of project: 1 January 2010
Ending date: 30 June 2012

Partner responsible for this deliverable: Siemens Corporate Research (SCR)



Revision 1

Project co-funded by the European Commission within the FP7	
Dissemination level	
RE	Restricted to a group specified by the consortium

	D5.2 Left Heart Model Extension	Sim-e-Child FP7-ICT-2009-4	(SeC)
--	---------------------------------	-------------------------------	-------

Document Classification

Title	Left Heart Model Extension and Delivery Report
Deliverable	D5.2.
Reporting Period	November 2010 – August 2011
Authors	Dime Vitanovski
Workpackage	WP5 - Development and Assessment of Personalized Child Heart Models
Security	Restricted
Nature	Report
Keywords	

Document History

Name	Remark	Version	Date
Dime Vitanovski	First draft	0.1	15/08/2011
Razvan Ionasec	Minor corrections	0.2	30/08/2011
Kristof Ralovich	Minor corrections	1.0	30/08/2011

Sim-e-Child Consortium

The partners in this project are:

01. Siemens AG (Siemens)
02. Lynkeus Srl (Lynkeus)
04. maat France (MAAT)
05. Technische Universität München (TUM)
06. I.R.C.C.S. Ospedale Pediatrico Bambino Gesù (OPBG)
07. Siemens Corporate Research, Inc. (SCR)
08. Johns Hopkins University (JHU)
10. American College of Cardiology Foundation (ACCF)
11. Siemens Program and System Engineering srl (PSE)

	D5.2 Left Heart Model Extension	Sim-e-Child FP7-ICT-2009-4	(SeC)
--	---------------------------------	-------------------------------	-------

List of contributors

Name	Affiliation	Co-author of
Razvan Ionasec	SCR	
Dime Vitanovski	Siemens	
Kristof Ralovich	TUM	

List of reviewers

Name	Affiliation
Michael Suehling	Siemens

	D5.2 Left Heart Model Extension	Sim-e-Child FP7-ICT-2009-4 (SeC)
--	---------------------------------	-------------------------------------

Table of Contents

1. INTRODUCTION..... 5

1.1. PURPOSE OF THE DOCUMENT 5

1.2. SCOPE OF THE DOCUMENT 5

1.3. REFERENCES 5

1.4. ABBREVIATIONS..... 6

2. MITRAL VALVE MODEL ESTIMATION FROM 2D+T MRI IMAGES 8

2.1. BRIEF OVERVIEW OF THE METHOD..... 8

2.2. MRI ACQUISITION PROTOCOL DEFINITION 8

2.3. REGRESSION-BASED MITRAL VALVE SURFACE RECONSTRUCTION..... 9

2.4. RESULTS..... 12

3. PATIENT-SPECIFIC ANATOMICAL MODEL ESTIMATION OF THE AORTA..... 14

3.1. BRIEF OVERVIEW OF THE METHOD..... 14

3.2. CLASSIFICATION-BASED COMPLETE AORTIC MODEL..... 14

RESULTS 15

3.3..... 15

4. PATIENT-SPECIFIC HEMODYNAMIC MODEL COMPUTATION OF THE AORTA... 17

4.1. BRIEF OVERVIEW OF THE METHOD..... 17

4.2. PATIENT-SPECIFIC AORTA FLOW ESTIMATION 17

4.3. PATIENT-SPECIFIC CFD OF AORTIC BLOOD FLOW 18

4.4. RESULTS..... 19

	D5.2 Left Heart Model Extension	Sim-e-Child (SeC) FP7-ICT-2009-4
--	---------------------------------	-------------------------------------

1. Introduction

The Sim-e-Child project proposes to develop a grid-enabled platform for large scale simulations in paediatric cardiology, providing a collaborative environment for constructing and validating multi-scale and personalized models of the growing heart and vessels. The objective of the Sim-e-Child is to strengthen the impact of the Health-e-Child project by creating an international simulation and validation environment for paediatric cardiology, supported by integrated data repositories. The project will advance the state-of-the-art by providing comprehensive and patient specific models for the dynamic and longitudinal interactions occurring in the left heart, with a focus on the congenital aortic arch disease and repair.

1.1. Purpose of the Document

The purpose of this document is to report on the extension of the Health-e-Child models for the left part of the heart. The left heart extension focuses on the mitral valve (MV) model and the complete aortic model (aortic root, ascending aorta, aortic arch and descending aorta) estimated from 3D and sparse 3D+t MRI images from patients affected by congenital heart disease. The results reported within this document are accepted as technical paper to be presented at the 14th International Conference on Medical Image Computing and Computer Assisted Intervention, Toronto, Canada 18-22 September, 2011.

1.2. Scope of the Document

This document presents the methods developed within the Sim-e-Child project to extend the Health-e-Child models for the left part of the heart. It is organized as follows:

- Section 1 introduces the developed regression-based algorithm for patient-specific mitral valve model estimation from 2D+t MRI images.
- Section 2 gives details about the hierarchical classification-based method developed to estimate patient-specific complete aortic model from 3D MRI images.
- In Section 3 we introduce how such estimated models can be used for personalized hemodynamic model computation.

1.3. References

[Vitanovski et al. 2011] Vitanovski, D., Tsymbal, A., Ionasec, R., Greiser, A., Schmidt, M., Mueller, E., Lu, X., Funke-Lea, G., Hornegger, J., Comaniciu, D., Accurate Regression-based 4D Mitral Valve Surface Reconstruction from 2D+t MRI Slices; in Machine Learning in Medical Imaging, MICCAI Workshop 2011.

[Ralovich et al. 2011] Ralovich, K., Ionasec, R. I., Mihalef, V., Georgescu, B., Everett, A., Navab, N., and Comaniciu, D., Computational Fluid Dynamics Framework for Large-Scale Simulation in Pediatric Cardiology; in Computational Biomechanics for Medicine VI (CBM6), MICCAI Workshop, 2011

[Vitanovski et al. 2010] Vitanovski, D., Tsymbal, A., Ionasec, R., Georgescu, B., Huber, M., Taylor, A., Schievano, S., Zhou, S.K., Hornegger, J., Comaniciu, D., Cross-modality Assessment and Planning for Pulmonary Trunk Treatment using CT and MRI Imaging; in MICCAI 2010.

	D5.2 Left Heart Model Extension	Sim-e-Child (SeC) FP7-ICT-2009-4
--	---------------------------------	-------------------------------------

[Mihalef et al. 2010] Mihalef, V., Ionasec, R., Wang, T., Zheng, Y., Georgescu, B., Comaniciu D. - Patient-specific modeling of left heart anatomy, dynamics and hemodynamics from high resolution 4D CT, Proceedings of ISBI 2010.

[Ionasec et al. 2009] Ionasec, R. I., Voigt, I., Georgescu, B., Houle, H., Navab, N., Comaniciu, D. Personalized Modeling and Assessment of the Aortic-Mitral Coupling from 4D TEE and CT; in International Conference on Medical Image Computing and Computer-Assisted Intervention (MICCAI)], 2009

[Mihalef et al. 2009] Mihalef, V., Metaxas, D., Sussman, M. , Hurmusiadis, V., Axel L. - Atrioventricular blood flow simulation based on patient-specific data, in Proceedings of FIMH 2009

[Ionasec et al. 2008] Ionasec, R. I., Georgescu, B., Gassner, E., Vogt, S., Kutter, O., Scheuering, M., Navab, N., and Comaniciu, D., Dynamic model-driven quantification and visual evaluation of the aortic valve from 4D CT; in International Conference on Medical Image Computing and Computer-Assisted Intervention (MICCAI)], 2008

[Zheng et al. 2008] Y. Zheng, A. Barbu, B. Georgescu, M. Scheuering, D. Comaniciu: Four-Chamber Heart Modeling and Automatic Segmentation for 3D Cardiac CT Volumes using Marginal Space Learning and Steerable Features, IEEE Trans. Medical Imaging, 2008

[Wang et al. 2007] Wang F, Bourgué PE, Hackenberg G, et al: “SciPort: An Adaptable Scientific Data Integration Platform for Collaborative Scientific Research”. Proc. VLDB, 1310-1313. 2007

[Zheng et al. 2007] Y. Zheng, A. Barbu, B. Georgescu, M. Scheuering, and D. Comaniciu. Fast automatic heart chamber segmentation from 3D CT data using marginal space learning and steerable features. In ICCV, 2007.

1.4. Abbreviations

CE-MRA	Contrast Enhanced MR angiography
CFD	Computational Fluid Dynamics
CT	Computed Tomography
DF	Desktop Fusion
DLL	Dynamic-link library
HeC	Health-e-Child
LA	Left Atrium
LV	Left Ventricle
MRI	Magnetic Resonance Imaging

	D5.2 Left Heart Model Extension	Sim-e-Child FP7-ICT-2009-4	(SeC)
--	---------------------------------	-------------------------------	-------

MSL	Marginal Space Learning
MV	Mitral Valve
PBT	Probabilistic Boosting Tree
RV	Right Ventricle
SeC	Sim-e-Child
TEE	Transesophageal Echo
UI	User Interface
US	Ultrasound
WSS	Wall Shear Stress

	D5.2 Left Heart Model Extension	Sim-e-Child (SeC) FP7-ICT-2009-4
--	---------------------------------	-------------------------------------

2. Mitral Valve Model Estimation from 2D+t MRI Images

2.1. Brief Overview of the Method

The multi-plane ability of MRI to acquire tomographic images in any plane, the capabilities to measure blood flow velocity in all three dimensions within a single slice and the non-ionizing radiation represent a significant advantage over other imaging modalities. However, estimating personalized valve models from standard MRI protocols is very challenging due to the slice-based imaging paradigm of MRI that may vary significantly across different application scenarios. To enable accurate and robust cardiac valve modeling, we have experimented with existing MRI protocols Siemens-internally by adapting them to optimize mitral valve model estimation. Based on these MRI acquisition protocol adaptations, we developed a novel regression-based method for patient-specific 4D MV model estimation. Based on extensive experiments on simulated data, we first defined the acquisition protocol and optimized it with respect to the number and spatial configuration of the 2D+t MRI slices resulting in reduced acquisition time and 4D MV estimation error. Second, we developed a novel regression-based algorithm to estimate a complete patient-specific mitral valve model from incomplete 2D+t MRI images. The main idea of our algorithm developed consists of learning a regression model from existing mitral valve models from other imaging modalities, CT and Ultrasound, which then can be utilized to estimate personalized MV models from 2D+t MRI images. *This work was submitted in a form of a technical paper and accepted as an oral presentation at the Machine Learning In Medical Imaging Workshop of the 14th International Conference on Medical Image Computing and Computer Assisted Intervention, Toronto, Canada 18-22 September, 2011.*

2.2. MRI Acquisition Protocol Definition

A Cardiac MR scanner (1.5T) with phased-array receiver coil and breath-hold acquisition was used to acquire cine images for MV function analysis. We covered the full cardiac cycle by using a retrospectively gated ECG signal. Data were collected during a multiple breath-holds (8 heart beats, slice thickness 4.5 mm, echo time 1.39 ms, pixel bandwidth 925 Hz, matrix 208x124, excitation angle 59 degree, field of view 276mm-340mm).

The mitral valve imaging plane was defined by acquiring four-chamber, three-chamber and short-axis view in the diastolic phase of the cardiac cycle. Initial orientation of the imaging plane is given by the short-axis view, where the plane normal passes through the MV commissures (Figure 1). Subsequently, parallel slices were defined along the normal between the commissures.

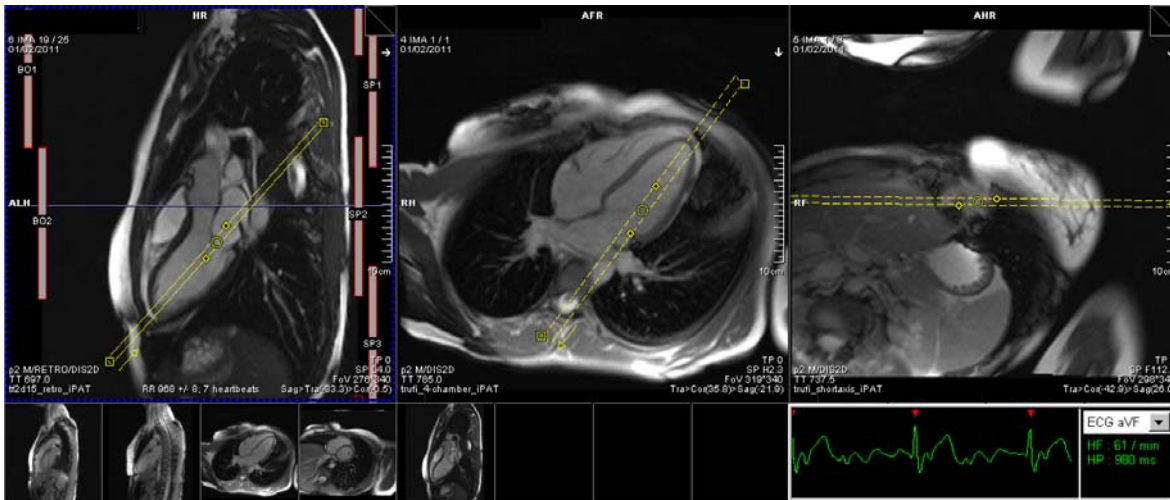


Figure 1: MRI Acquisition Protocol Definition

Within this study we also exam the best trade-off between MV model estimation error and acquisition time by experimenting with different MRI imaging protocols on simulated data. For the different MRI acquisition protocols we estimated the mitral valve model in the end-diastolic (ED) and end-systolic (ES) cardiac phases. Based on the experiments from the simulated data (see Table 1) a stack of 6 parallel LA planes results in best trade-off between MV model estimation error and acquisition time. We also considered a protocol with 6 radial LA planes as an option. However, due to the long acquisition planning time, the complicated plane settings and the plane mis-registration characteristic for this acquisition protocol, we found that a stack of 6 parallel planes is more appropriate for MV model estimation.

No. Planes	2	3	4	5	6	7	8	9	10
ED (mm)	6.7±1.1	5.6±1.0	4.4±0.9	3.5±0.68	3.1±1.1	2.6±1.0	2.3±1.0	2.1±1.0	1.8±0.8
ES (mm)	2.9±1.2	2.6±2.2	2.2±1.5	2.1±1.4	2.1±1.2	2.3±1.6	2.5±2.3	2.1±1.1	1.9±1.0

Table 1: MRI acquisition protocol optimization: analyzing the reconstruction error for different number of MRI imaging planes defined parallel between the MV commissures.

2.3. Regression-Based Mitral Valve Surface Reconstruction

The regression-based algorithm for complete mitral valve model estimation from sparse 2D+t MRI images consists of a hierarchical workflow, from modeling to quantification, which includes three stages: landmark detection (Figure 3), detection of contours (Figure 3) and model estimation (Figure 4). In order to accurately represent morphology and dynamics, our model design is consistent with the anatomy and physiology of the mitral valve (Figure 2). The architecture of the model is anatomy-based and includes all clinical relevant structures. In the following detailed introduction of our idea, developed algorithms and workflow supported by the User Interface integrated into SimSys are introduced.

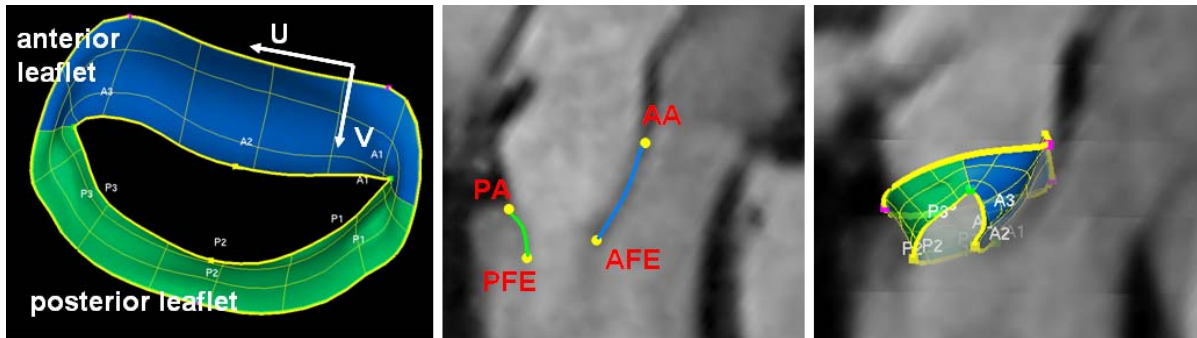


Figure 2: Morphological and physiological representation of our mitral valve model

Stage 1: Mitral Valve Landmarks Estimation. [Lu et al. 2010] proposed a framework for landmarks detection from 2D MRI images by their joint context. In our mitral valve landmarks detection phase from 2D+t parallel oriented MRI images we define our joint context landmark set between the posterior annulus and the free edge landmarks (PA, PFE) and the anterior leaflet (AA, AFE), respectively (Figure 2(middle)). On each 2D MRI slice we apply the developed 2D landmark classifiers, trained with PBT [Tu et al. 2005] and 2D Haar-like features to detect the annulus and free edge landmarks independently. Furthermore, we have integrated in the SimSys platform a graphical user interface which simultaneously displays all 6 MRI images fused with the estimated landmarks and provides the user interactive correction of sub optimally estimated landmarks (Figure 3).

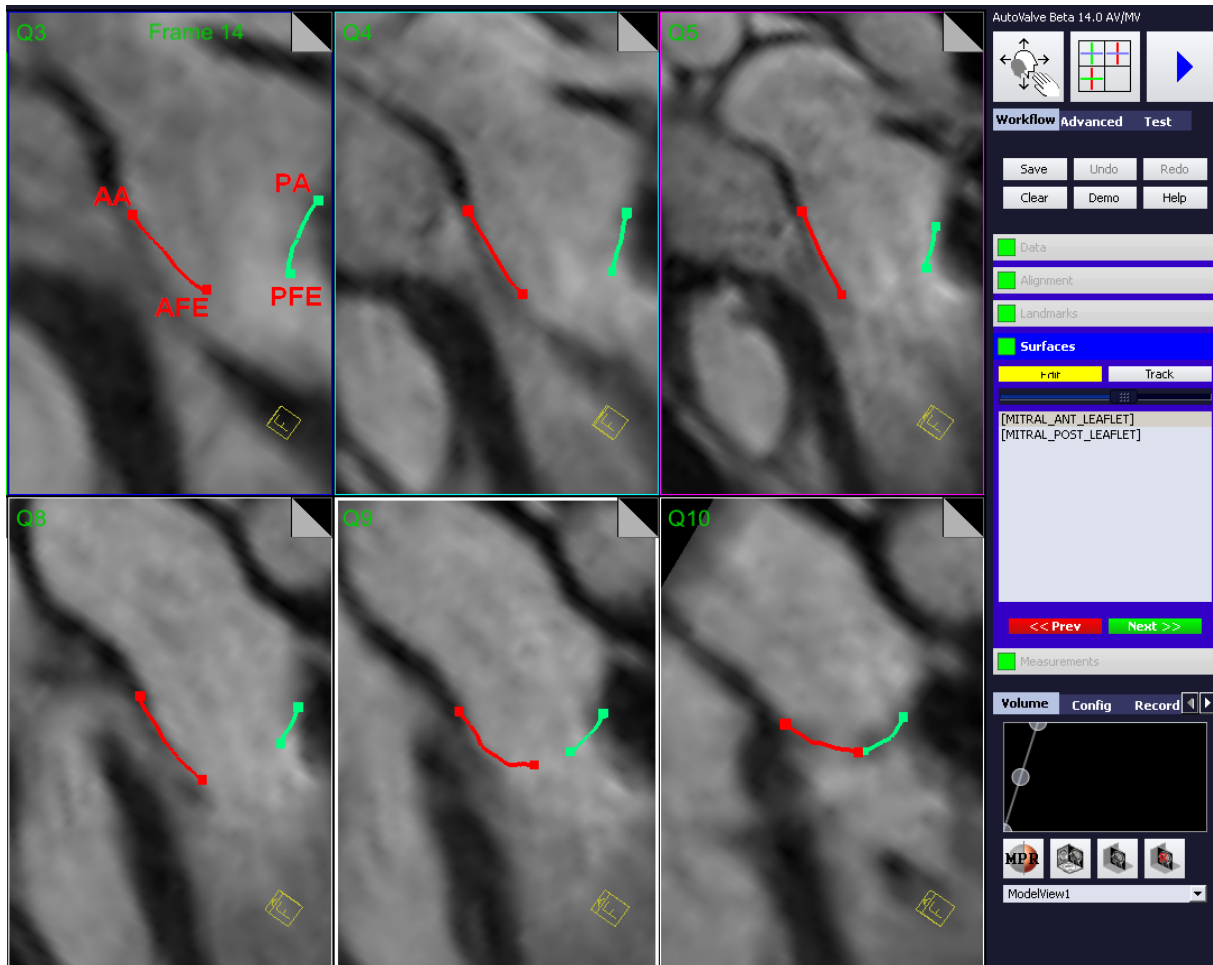


Figure 3: Graphical user interface integrated into SimSys platform for interactive correction of badly estimated landmarks or contours

Stage 2: Mitral Valve *Contours* Estimation. From previously detected landmarks, we initialize the contours, parameterized by 17 discrete points, as a straight line and search for edges along the normal. A least-squares approach is used to fit a parametric NURBS curve to the discrete set of detected contour points. An interactive graphical UI of the SimSys platform allows the correction of incorrectly estimated contours by the user (Figure 3).

Stage 3: Mitral Valve *Model* Estimation. In the last stage of the hierarchical mitral valve model estimation workflow, we incorporate the detected landmarks and contours from each cardiac phase (t) into the learned regression model. As a result a full patient-specific mitral valve model is estimated over the cardiac cycle from six parallel 2D+t MRI images. Figure 4 illustrates an example of the estimated mitral valve model together with quantitative analysis of the valve and annulus area over the cardiac cycle.

$$Model_{MV} = \mathfrak{R}(\text{Landmarks}, \text{Contours}) + \varepsilon$$

Equation 1: Mathematical representation of the regression based MV model estimation

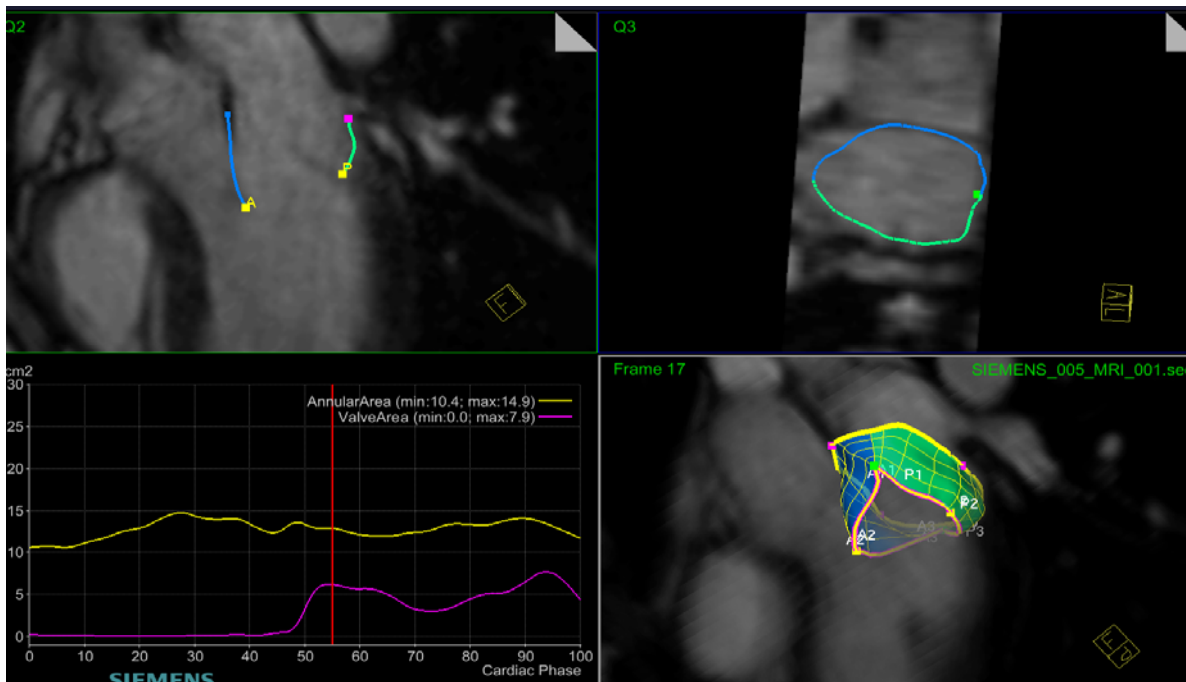


Figure 4: Personalized mitral valve model regressed from six parallel oriented 2D+t MRI slices.

2.4. Results

We evaluated the developed algorithm for personalized 4D MV model estimation in sparse MRI data on a large set of simulated data (200 US TEE and 20 cardiac CT sequences) and on 15 ECG gated MRI studies acquired according to our developed protocol. Each volume in the data set is associated with annotation, manually generated, which is considered as ground truth for the learning algorithm. The personalized MV model estimation accuracy was evaluated by using the point-to-mesh metric. For each point of the estimated model we compute the Euclidean distance to the closest point of the associated, manually generated, ground-truth model.

Intra and inter modality accuracy of the developed method with respect to different algorithm settings and parameters was evaluated. The inter modality accuracy was evaluated by learning the regression model on images simulated from US TEE data and tested on simulated sparse 2D+t images from CT data. For the intra modality accuracy a 3-fold cross validation was used to divide the US TEE data set into training (used to learn the regression model) and test data (used to evaluate the model estimation accuracy). For the best plane configuration protocol (stack of 6 parallel images) we achieved mitral valve model estimation accuracy of 1.9 ± 0.5 mm for the intra modality evaluation and 2.3 ± 0.5 mm for the inter modality. The intra and inter modality evaluation was important for two reasons: we had to prove our concept of cross-modality learning and we had to exam the best configuration of the imaging planes before we start to acquire real MRI data.

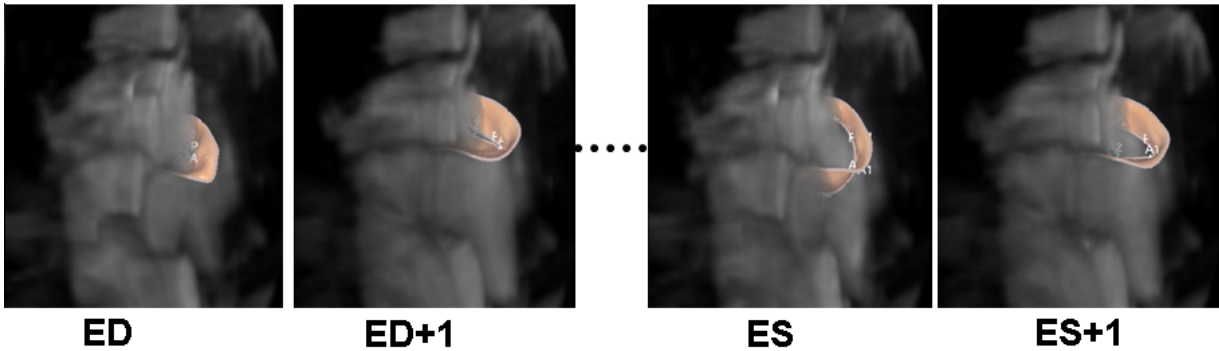


Figure 5: Example of the reconstructed 4D MV model over the cardiac cycle from 6 parallel 2D+t MRI slices which only partially cover the MV anatomy.

With the results of the inter modality accuracy we prove the applicability of the MV anatomical model across different imaging modalities. In addition, we have shown that a regression model can be learned from one imaging modality (US) and used to estimate a patient-specific MV model in other imaging modality (CT). Finally, the regression model was learned with the best parameter configuration on all available US and CT data (1295 3D volumes). We then applied the learned regression model to estimate patient-specific MV models from the 15 MRI studies acquired according to the developed protocol and evaluate the model estimation accuracy by computing the point-to-mesh distance between the estimated and the associated ground-truth model. Our method achieved MV model estimation accuracy of 1.5 ± 0.2 mm within 10 sec per volume. Figure 5 illustrates the estimated MV models for the ED and ES phase of the cardiac cycle for the 2D+t MRI studies.

	D5.2 Left Heart Model Extension	Sim-e-Child (SeC) FP7-ICT-2009-4
--	---------------------------------	-------------------------------------

3. Patient-Specific Anatomical Model Estimation of the Aorta

3.1. Brief Overview of the Method

Within the SeC project we have developed hierarchical three-stage classification-based method for estimating patient-specific models of the aorta. We learned classifiers with PBT [Tu et al. 2005] and MSL [Zheng et al. 2007, Ralovich et al. 2011] to first localize the aortic root and arch in given 3D MRI volume, then to determine the center line along the aorta and finally to estimate the patient-specific aortic model (Figure 6). The estimated model provides a better understanding of the geometry of the aortic anomaly, especially in coarctation and bicuspid aortic valve patients, and can be utilized during preoperative planning. *This work was submitted in a form of a technical paper and accepted as an oral presentation at the Computational Biomechanics for Medicine VI Workshop of the 14th International Conference on Medical Image Computing and Computer Assisted Intervention (MICCAI), Toronto, Canada 18-22 September, 2011.*

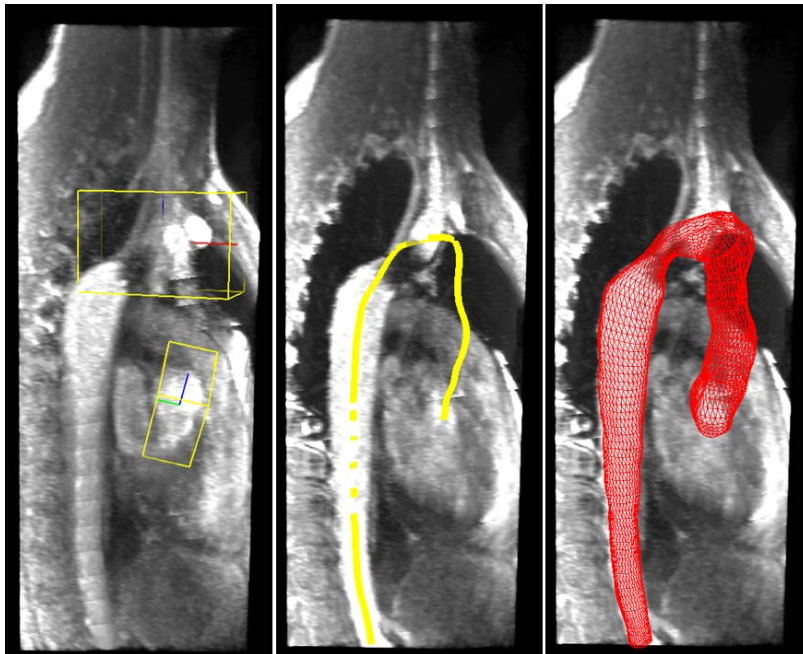


Figure 6: Hierarchical aortic model estimation workflow. (Left) Aortic root and arch localization phase. (Middle) Centre line extraction step. (Right) Aortic model fitted into the patient-specific MRI anatomy.

3.2. Classification-Based Complete Aortic Model

In SeC we employ a part-based aorta model (as shown in Figure 7) by splitting the whole aorta into four parts: aortic root, ascending aorta, aortic arch, and descending aorta similar to [Zheng et al. 2010]. The aortic root is required to be present in SeC image data; therefore, it is detected and segmented as the first step. More specifically, we use the recently proposed marginal space learning (MSL) method to segment the aortic root. MSL is an efficient method to detect and segment a 3D anatomical structure in medical images based on a robust discriminative machine learning technique. As shown in the system diagram in **Fehler!**

Verweisquelle konnte nicht gefunden werden., the aortic root is detected first. If no aortic root is detected, the input volume is rejected. We then detect the aortic arch. Similarly, MSL is exploited to train a separate detector for the aortic arch. The length of the ascending and descending aorta segments captured in a volume varies significantly. It is difficult to detect them as whole objects. Therefore, we propose to use a tracking technique to deal with this variation. Since the intersection of the ascending and descending aorta segments with an image slice is close to a circular shape, we train a 2D circle detector using Haar wavelet features and the boosting learning algorithm to detect aortic circles as primitive structures for tracking. Starting from the aortic root, we detect an aortic circle on the next slice (toward the patient's head). The detector outputs multiple circle candidates around the true position. We pick the one closest to the circle on the current slice. If the aortic arch is detected in the volume, the tracking procedure stops on the slice touching the aortic arch. Otherwise, it stops when no aortic circle is detected or it reaches the top volume border. Tracking of the descending aorta is similar except that it starts from the aortic arch and moves toward the patient's toe. It stops on the slice with no aortic circle detected.

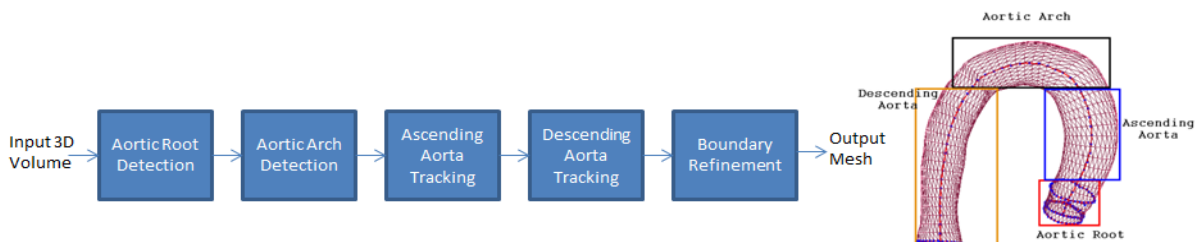


Figure 7: Part-based aorta model (right) and automatic segmentation workflow (left)

3.3. Results

Timing and type of surgical or catheter-based repair of aortic wall complications (AWC) in patients with aortic coarctation (COA) and/or bicuspid aortic valve (BAV) are presently being debated, as associated morbidity and mortality can still occur. Automatic, patient-specific 3D aortic arch model estimation from MRI images provides a better understanding of the geometry of the aortic arch anomaly and might be utilized to evaluate preoperatively the best treatment. Clinicians from JHU and OPBG validated the accuracy of the estimated patient-specific 3D aortic model by comparing manual with model-based derived aortic measurements.

The system performance is demonstrated on 32 patients with aortic arch anomalies (age: 5-36 years), 17 with COA and 15 with BAV and ascending aorta dilation. The aortic arch min and max diameter were measured manually from 3D SSFP MRI sequence at aortic sinus (AS), sino-tubular junction (STJ), ascending aorta (AAO), transverse arch (TA), and descending aorta (DA). Measurements at the same regions were automatically derived from the computer-based model for each patient.

Statistical results significantly correlated ($p < 0.001$, $r = 0.94$) between min and max manual and automatic aortic measurements: AS (min $p < 0.001$ $r = 0.85$; max $p < 0.001$ $r = 0.94$), STJ (min $p < 0.001$ $r = 0.88$; max $p < 0.001$ $r = 0.90$), AAO (min $p < 0.001$ $r = 0.94$; max $p < 0.001$

	D5.2 Left Heart Model Extension	Sim-e-Child FP7-ICT-2009-4 (SeC)
--	---------------------------------	-------------------------------------

$r = 0.94$), TA (min $p < 0.001$ $r = 0.89$; max $p < 0.001$ $r = 0.93$), DA (min $p < 0.001$ $r = 0.90$; max $p < 0.001$ $r = 0.92$).

Mean measurement error of 1.59 ± 0.6 mm was achieved for the min diameter and 1.44 ± 0.9 mm for the max diameter. The maximal error occurred at the minimum diameter of each segment with the STJ the greatest (min 2.07 ± 2.53) and the DA the least (min 0.8 ± 0.83).

Mean processing time for fully-automatic aortic model estimation and measurement extraction was 1.5 s.

Our fully-automated method for personalized aortic model estimation markedly reduced the time necessary to complete volumetric assessment of the aorta. From the results, we have concluded that the aortic measurements automatically derived from our model are reliable, fully-reproducible and faster as compared to manual methods. The developed system for 3D aortic model estimation can be useful tool to improve therapeutic decision making in COA and/or BAV patients.

	D5.2 Left Heart Model Extension	Sim-e-Child (SeC) FP7-ICT-2009-4
--	---------------------------------	-------------------------------------

4. Patient-Specific Hemodynamic Model Computation of the Aorta

4.1. Brief Overview of the Method

We have developed a unified computational framework for large-scale hemodynamic modelling and simulations to aid diagnostic and therapy decision making. Our method provides a deterministic and streamlined processing pipeline to perform Computational Fluid Dynamics (CFD) simulations from the estimated patient-specific models. The developed method includes an automated approach to segment the inlet and outlet flow profiles over the entire cardiac cycle. CFD simulations are performed using an embedded boundary method solved within a level-set formulation. *This work was submitted in a form of a technical paper and accepted as an oral presentation at the Computational Biomechanics for Medicine VI Workshop of the 14th International Conference on Medical Image Computing and Computer Assisted Intervention (MICCAI), Toronto, Canada 18-22 September, 2011.*

4.2. Patient-Specific Aorta Flow Estimation

In the aorta flow estimation phase we extract the patient-specific flow profiles over the entire cardiac cycle at the aortic inflow and outflow from the 2D PC-MRI cine images. Typically, the PC-MRI sequence is easily registered with the anatomy image and aortic segmentation using the MR machine coordinates. The intersection of the PC-MRI image plane and the vessel geometry defines two 2D closed contours. These planar patches are densely triangulated and treated as an inflow and outflow profile, respectively. Inside each patch a uniform grid sampling of the PC-MRI image is performed at the pixel centre locations to obtain spatially constrained velocity values over the entire cardiac cycle (Figure 8). The whole simulation pipeline is illustrated in Figure 9.

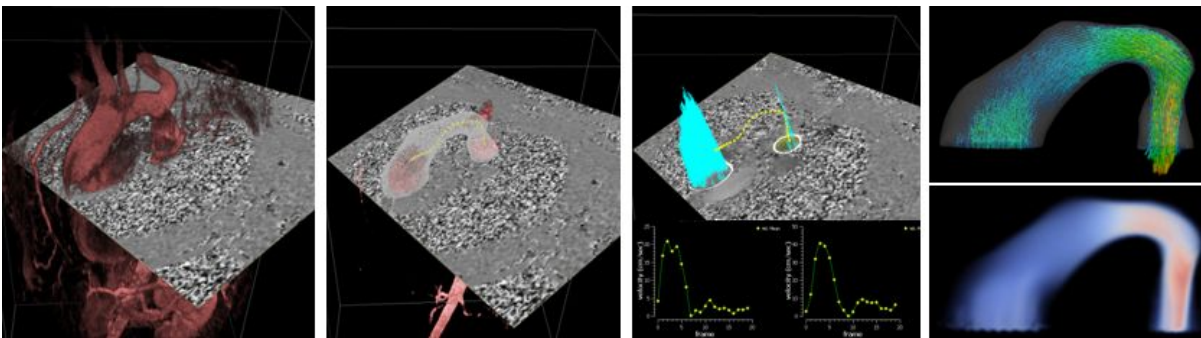


Figure 8: Pipeline of the simulation: (a) Volume rendering of a clear, high contrast CE-MRA image displayed together with a PC-MRI slice used for depicting an aortic arch. (b) Extracted centerline and segmentation of the aorta (c) Patient specific systolic in- and outflow rates derived from PC-MRI measurement. (d) Simulated blood flow velocities and vorticity magnitude.

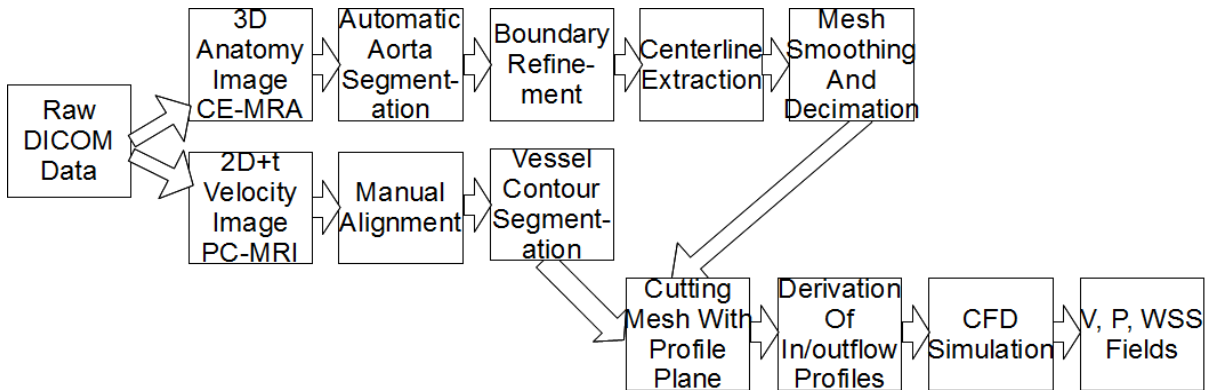


Figure 9: Detailed CFD simulation pipeline

4.3. Patient-Specific CFD of Aortic Blood Flow

We model the blood flow dynamics in the aorta using 3D incompressible Navier-Stokes equations with viscous terms – the standard continuum mechanics model for fluid flow. The equations are discretized and solved with the embedded boundary method. We use both finite difference and finite volume techniques to solve the fractional step combined with an approximate projection method for the pressure. The blood is modelled as a Newtonian fluid, which is generally accepted as a reasonable first approximation to the actual behavior of blood at shear rates observed in large arteries.

The boundary conditions used in the simulations are as follows: at the aortic walls we use no-slip for the velocity and the appropriate normal balance (translating into a Neumann boundary condition) for the pressure. The inflow velocity is extrapolated from the MRI, using smooth kernels, to all the inlet nodes, while pressure proportional to the flow is set as a Dirichlet boundary condition on the outlet faces. The inflow velocities are also interpolated in time using second order accurate interpolation.

The developed algorithm starts at a given time step n from the velocity and pressure information at the previous time step u^{n-1} , p^{n-1} and computes u^n , p^n following a fractional step projection. Figure 10 summarizes the computation setup together with CFD visualization results.

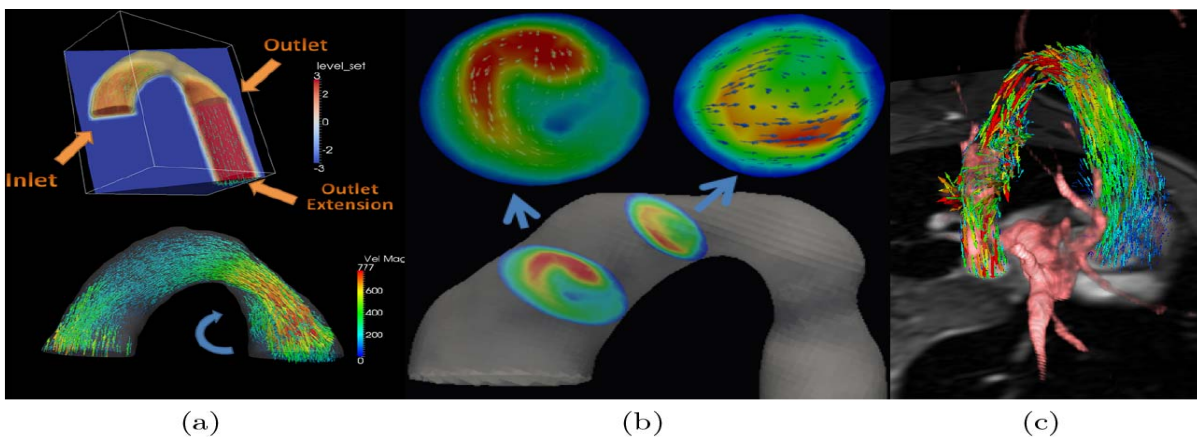


Figure 10: (a) our computational setup: the Lagrangian aortic mesh is embedded in an Eulerian domain using level set. Visible here are a cross-section of the domain, color-coded with the

level set values, and the embedded aortic mesh (in transparent yellow) together with its outlet extension (in transparent white). The blood flow velocity field during early systole, simulated using CFD, is also visualized as a vector field. Below, coarctation with vortex formation. (b) Enhanced helical rotation due to bicuspid valve. (c) Simulation results overlaid with anatomical images.

4.4. Results

With the developed CFD simulation framework we have performed a series of simulations using the geometric constraints of the aortic meshes as static boundary conditions, and the sampled MRI-derived velocity as the inflow profiles. The aortic data was selected from patients with various pathologies, including bicuspid valve, coarctation, artificial valves and stents. We will give here an outline of several observed patterns that correlate with the various pathologies.

The cardiac cycle simulated using our CFD method features generic flow patterns like waveform delay between inlet and outlet, or increased velocities in the aortic arch. Furthermore, with our method, we also recover patterns specific to various pathologies, as outlined below. A first experiment used aortic data featuring medium coarctation in the descending region. The vortex formation pattern specific to coarctation was observed, and is shown in Figure 10. A bicuspid heart experiment (Figure 10 (b)) produced the enhanced helical pattern observed in such hearts, due to the blood jet that hits the aortic wall in the lower ascending aorta. Figure 11 gives one example of estimated patient-specific flow together with its aortic model.

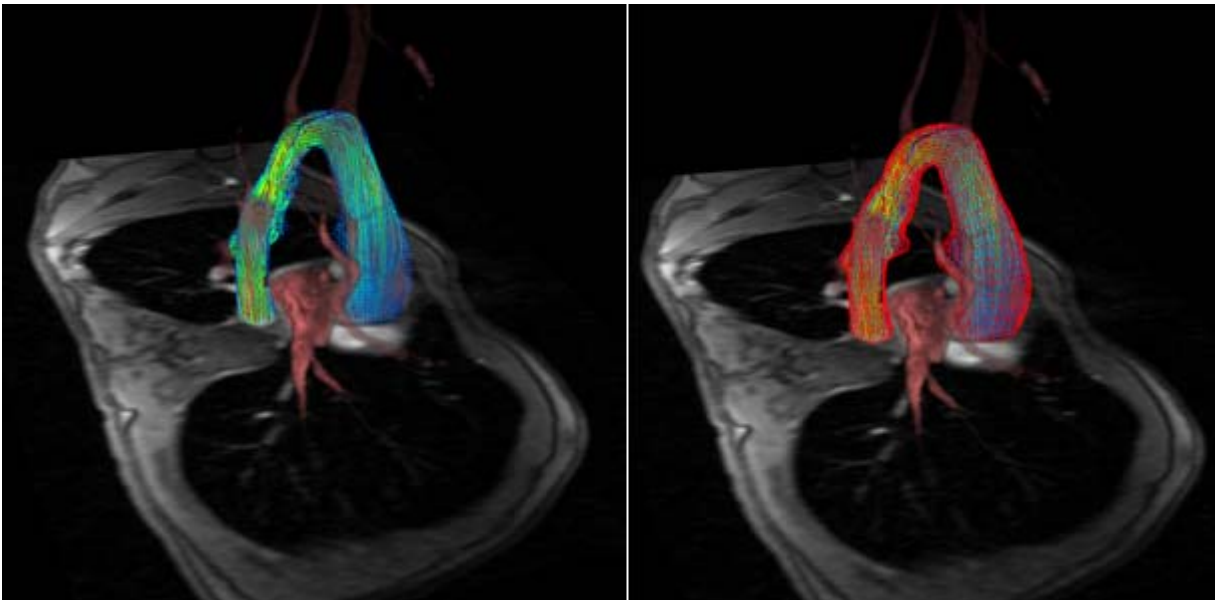


Figure 11: Example of an estimated patient-specific flow (left) and its aortic model (right)